




# The real Nemo movie: Description of embryonic development in *Amphiprion ocellaris* from first division to hatching

Pauline Salis<sup>1,2</sup>  | Shu-hua Lee<sup>3</sup> | Natacha Roux<sup>1</sup>  | David Lecchini<sup>2</sup> | Vincent Laudet<sup>3,4</sup> 

<sup>1</sup>Observatoire Océanologique de Banyuls-sur-Mer, UMR CNRS 7232 BIOM, Sorbonne Université Paris, Banyuls-sur-Mer, France

<sup>2</sup>EPHE-UPVD-CNRS, USR 3278 CRIOBE, PSL University, Moorea, French Polynesia

<sup>3</sup>Lab of Marine Eco-Evo-Devo, Marine Research Station, Institute of Cellular and Organismic Biology, Academia Sinica, Taipei, Taiwan

<sup>4</sup>Marine Eco-Evo-Devo Unit, Okinawa Institute of Science and Technology, Onna son, Okinawa, Japan

## Correspondence

Vincent Laudet, Lab of Marine Eco Evo Devo, Marine Research Station, Institute of Cellular and Organismic Biology, Academia Sinica, Taipei, Taiwan.  
Email: vincent.laudet@oist.jp

## Funding information

Agence Nationale de la Recherche, Grant/Award Numbers: ANR-19-CE14-0010-SENSO, ANR-19-CE34-0006-Manini

## Abstract

**Background:** *Amphiprion ocellaris* is one of the rare reef fish species that can be reared in aquaria. It is increasingly used as a model species for Eco-Evo-Devo. Therefore, it is important to have an embryonic development table based on high quality images that will allow for standardized sampling by the scientific community.

**Results:** Here we provide high-resolution time-lapse videos to accompany a detailed description of embryonic development in *A. ocellaris*. We describe a series of developmental stages and we define six broad periods of embryogenesis: zygote, cleavage, blastula, gastrula, segmentation, and organogenesis that we further subdivide into 32 stages. These periods highlight the changing spectrum of major developmental processes that occur during embryonic development.

**Conclusions:** We provide an easy system for the determination of embryonic stages, enabling the development of *A. ocellaris* as a coral reef fish model species. This work will facilitate evolutionary development studies, in particular studies of the relationship between climate change and developmental trajectories in the context of coral reefs. Thanks to its lifestyle, complex behavior, and ecology, *A. ocellaris* will undoubtedly become a very attractive model in a wide range of biological fields.

## KEYWORDS

coral reef fish, developmental stages, embryogenesis, pigmentation, Pomacentridae, time-lapse video

## 1 | INTRODUCTION

Developmental biology is built around model organisms such as the mouse *Mus musculus*, the chicken *Gallus gallus*, the frog *Xenopus laevis*, the zebrafish *Danio rerio*, the

Pauline Salis and Shu-hua Lee these authors contributed equally.

This is an open access article under the terms of the Creative Commons Attribution-NonCommercial License, which permits use, distribution and reproduction in any medium, provided the original work is properly cited and is not used for commercial purposes.

© 2021 The Authors. *Developmental Dynamics* published by Wiley Periodicals LLC on behalf of American Association of Anatomists.

fruit fly *Drosophila melanogaster*, and the round worm *Caenorhabditis elegans*. However, such model organisms, sometimes called “supermodels,” only represent a very small and biased fraction of living biodiversity and can therefore limit our understanding of the diversity of biological processes.<sup>1</sup> There is a widely recognized need for additional model species that better represent the diversity of the animal kingdom. Recently, the development of tools such as massive sequencing and CRISPR/Cas9 have rendered this possible.<sup>2</sup>

Diversity is particularly lacking in the teleost fishes, for which zebrafish, and to a lesser extent medaka (*Oryzias latipes*), have emerged as invaluable model species, complete with elaborate technological tools and a vivid scientific community.<sup>3,4</sup> However, these two species do not represent the diversity of the ca. 30 000 species of teleost fishes.<sup>5</sup> Several additional models have emerged in recent years (1990-2010) such as the stickleback, *Gasterosteus aculeatus*, the cichlids (eg, the tilapia, *Oreochromis niloticus*), the poeciliid fishes (eg, guppies and platys), the annual killifishes, and the *Astyanax mexicanus* cavefish.<sup>6-10</sup> These models, whose embryonic development has been well described,<sup>11-14</sup> have shed new light on a number of relevant biological questions. But they suffer from a limit: they are mostly freshwater fishes and capture only a fraction of teleost fishes diversity. The majority of teleosts are marine,<sup>5</sup> but, mostly because of

their biphasic life cycle (with extremely numerous small eggs and tiny pelagic larvae that will metamorphose into juveniles), they are notoriously difficult to raise in captivity at the laboratory scale. To date, only a few studies have examined embryogenesis in marine fishes, including flatfish, sea bream, sea bass, mahi-mahi, and grouper (see eg,<sup>15,16</sup>), limiting our ability to address a wide range of biological questions in this group.<sup>17-19</sup>

In our lab, we are working to develop the false clownfish *Amphiprion ocellaris* as a marine teleost fishes model system.<sup>20</sup> Living in symbiotic association with giant sea anemones, this species is native to the Indo-West Pacific region from the Ryukyu Islands in Japan to northwestern Australia. Like most coral reef fishes, *A. ocellaris* have a biphasic life cycle with a dispersive oceanic phase and a more sedentary reef phase (Figure 1). In contrast to many coral reef fishes that spawn in the open ocean, false clownfishes are benthic spawners.<sup>20</sup>

*A. ocellaris* are an ideal model for studies of embryogenesis because breeding pairs spawn regularly, laying 100 to 300 eggs every 2 weeks, and because the chorion is transparent until hatching, allowing for visualization of ongoing embryonic development.<sup>21,22</sup> Classical techniques of developmental biology, including in situ hybridization, have been successfully performed on false clownfish embryos.<sup>23</sup> This fish is therefore a new model species with a high potential for further study of

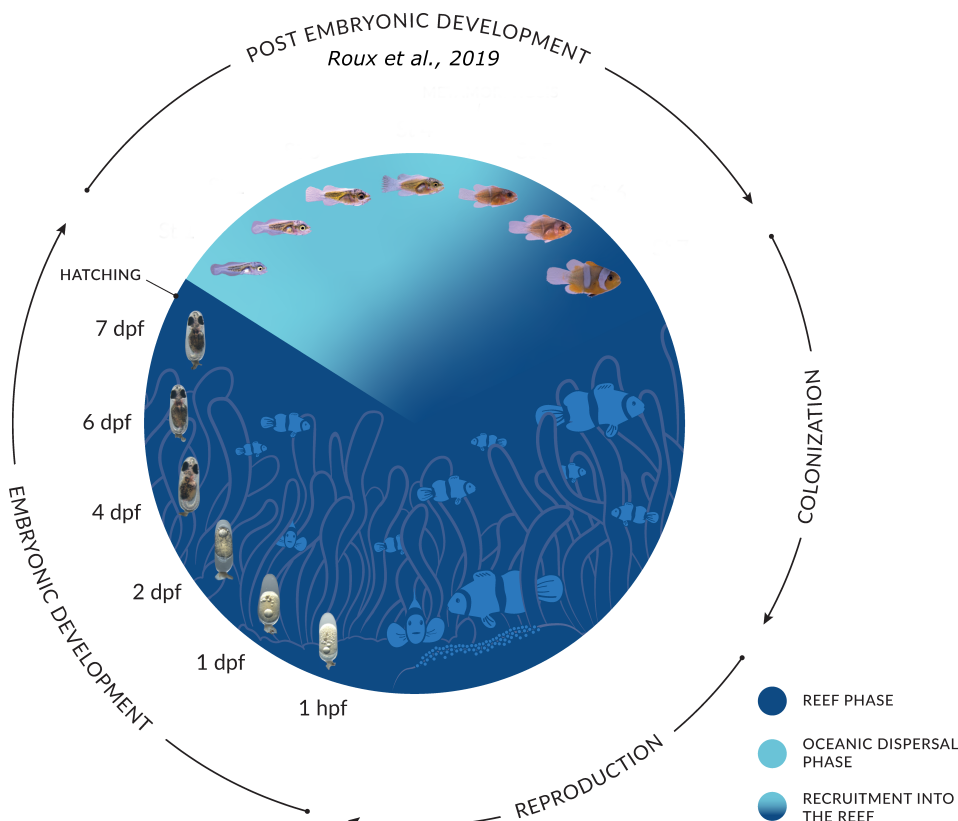


**FIGURE 1** Life cycle of *A. ocellaris*. *A. ocellaris* lay their eggs close to their sea anemone, where they will develop for 6 to 10 days, depending on temperature. After hatching, larvae are directly dispersed into the open ocean, where they will grow for 10 to 15 days before returning to the reef. Larval development is characterized by seven distinct stages.<sup>33</sup> The transition between the ocean and the reef is associated with the metamorphosis of larvae into juveniles. Juveniles will then settle into a sea anemone



evolutionary and developmental processes in a unique ecological framework. Other anemone fish species, and in particular the sister species *Amphiprion percula*, have also been used as model species<sup>24–26</sup> although to our knowledge *A ocellaris* is the most widely used at present.

*A ocellaris* belongs to a monophyletic group of 30 species, the anemonefishes (subfamily Amphiprioninae) within the family Pomacentridae (Teleostei; Perciformes; Pomacentridae;<sup>27</sup>). These fish provide an excellent example of rapid adaptation, fast speciation, and parallel evolution.<sup>28</sup> The symbiotic association with sea anemones (considered to be an obligate mutualistic relationship) is thought to have been the key innovation that allowed anemonefishes to radiate rapidly in untapped ecological niches.<sup>29</sup> As expected under the ecological theory of adaptive radiation, this increased diversification, rates of morphological evolution,<sup>30</sup> and rapid and convergent morphological changes correlated with the different ecological niches offered by different host anemones.<sup>28</sup> Thus, anemonefishes allow us to integrate studies of ecology, genomics, and development (eco-evo-devo) to understand adaptive radiation and phenotypic divergence.<sup>20</sup>

Establishing a precise and well-illustrated embryonic developmental table for this species would therefore be of particular interest. Developmental staging is essential because heterogeneity among individuals means that age does not perfectly correlate with development.<sup>31</sup> Staging tables are available for most model organisms (eg, zebrafish<sup>32</sup>). Here, we provide high resolution pictures and time lapse videos of false clownfish embryonic development and describe with high accuracy developmental stages that can be used by the scientific community. We define six broad periods of embryogenesis: zygote, cleavage, blastula, gastrula, segmentation, and organogenesis. These periods highlight the major developmental processes that occur between fertilization and hatching. Stages subdivide the periods and are based on morphological features readily identified by examination of the live embryo with a dissecting stereomicroscope. In a previous paper, we described the post-embryonic stages<sup>33</sup>; together these papers detail the entirety of development from fertilization to recruitment into a sea anemone in *A ocellaris*.

## 2 | RESULTS

### 2.1 | General description

The embryonic phase occurs directly after fertilization and lasts until hatching; this takes six to 10 days in false clownfishes, depending on temperature (between 25°C and 29°C). After hatching, larvae are directly dispersed

into the open ocean, where they grow for 10 to 15 days before returning to the reef. The transition between the ocean and the reef is associated with the metamorphosis of larvae into juveniles that will settle into a sea anemone.

We document in detail the development of the false clownfish *A ocellaris*, which in aquaria lasts for 7 days at 26°C (in our conditions) from fertilization to hatching. In addition to pictures allowing recognition of standardized periods and stages, we provide high resolution videos that fully illustrate the dynamics of development. These videos are available as supplementary material.

To look at embryonic development more broadly, we group the 32 developmental stages into six larger time-blocks that we call periods: zygote, cleavage, blastula, gastrula, segmentation, and organogenesis (Figure 2). Table 1 summarizes brief descriptions of the main morphological changes occurring at each stage. Figure 2 shows overall development and highlights the six periods. It also shows the corresponding available time-lapse movies.

### 2.2 | Zygotic period

In our facility, the female lays eggs on a terracotta pot. Once the female has spawned, she leaves the nest, and the male fertilizes the eggs. Newly fertilized eggs of *A ocellaris* have an ovoid shape, with the longitudinal axis ( $1.707 \pm 0.037$  mm) longer than the transverse axis ( $0.872 \pm 0.019$  mm) (Figure 3A). The egg is surrounded by a translucent envelope called the chorion. The fertilized cell is located at the end of the egg closest to the adhesive edge of the chorion (Figures 3A and A'). False clownfish eggs are telolecithal with the yolk concentrated at the vegetal pole. The yolk is composed of large dark-yellow yolk globules/platelets, giving it a grainy appearance. After spawning, the chorion sticks to the terracotta pot through a mucous secretion (Figure 3A, A').

**One-cell stage (0 hpf):** Fertilization induces an increase in the volume of the blastodisc which replaces the yolk (Figure 3A, A', B, B'). The blastodisc gradually segregates from the yolk and forms a more prominent cell (Figure 3B, B', Movie 1).

### 2.3 | Cleavage period

We define the cleavage period as consisting of six stages: 2-, 4-, 8-, 16-, 32-, and 64-cell stages (Figures 2 and 3). Cleavages are synchronous and occur every 30 min at 26°C. As in most teleost fishes, they are meroblastic

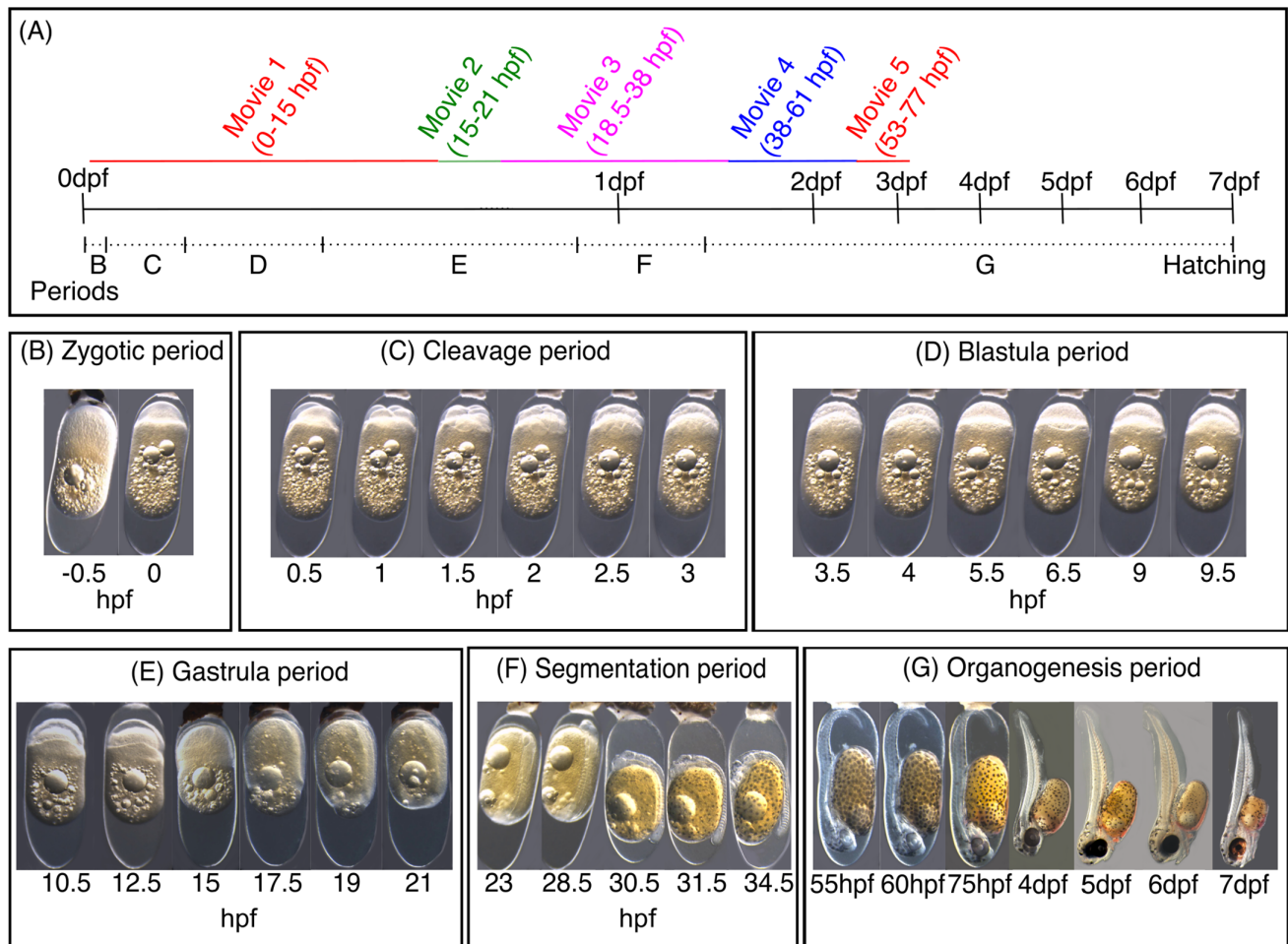


**FIGURE 2** Time scale of periods and stages from zygotic period until hatching. (A) Time scale of the important steps of *A. ocellaris* embryonic development at 26°C, and the movies associated with: (B) Zygotic period; (C) Cleavage period; (D) Blastula Period; (E) Gastrula period; (F) Segmentation period; (G) Organogenesis period. Dpf, days post fertilization; hpf, hours post fertilization

(incomplete) and discoidal (ie, that they only occur in the blastodisc which keep a connection with the yolk). Early cleavage divisions follow a highly reproducible pattern of meridional and equatorial planes (Figure 3I).

**Two-cell stage (0.5 hpf):** The first cleavage furrow, ending the first zygotic cell cycle, is vertically oriented (Figure 3I) dividing the blastodisc into two cells (blastomeres) of equal size. This pattern is seen in other teleost species until the 32-cell stage.<sup>11-14,32</sup> Both cells stay connected to the underlying yolk (meroblastic cleavage) (Figure 3C and C', Movie 1).

**Four-cell stage (1 hpf):** In the second division, the cleavage plane is oriented perpendicular to the first one, resulting in four blastomeres arranged in a 2 X 2 array when viewed from the animal pole (Figure 3D and D', I, Movie 1).

**Eight-cell stage (1.5 hpf):** The third set of cleavages occurs in two planes parallel to the first cleavage plane, dividing the four blastomeres into eight blastomeres.

They are arranged in a 2 X 4 array (Figure 3E, E', I, Movie 1).

**16-cell stage (2 hpf):** The fourth cleavage also occurs along two planes, this time parallel to the second cleavage plane. The two rows of four blastomeres are divided into four rows of four blastomeres (4 X 4 array) (Figure 3F, F', I, Movie 1).

**32-cell stage (2.5 hpf):** The fifth set of cleavages generates a 4 X 8 array of cells, although the pattern is less stereotypic than in previous stages. All cells are still in contact with the yolk, shaping the underlying yolk into a dome-like structure (Figure 3G, G', Movie 1).

**64-cell stage (3 hpf):** During the sixth set of divisions, cells start to be cleaved completely from the others, forming a second layer of cells on top of those that are still connected to the yolk (marginal cells). Unlike in previous stages, there are no regularly-patterned cleavage planes or stereotypical cell arrangements (Figure 3H, H', Movie 1).

TABLE 1 Stages of embryonic development

Stage	Figure	Movie	Hpf	Description
<b>Zygotic period</b>				
Zygotic stage	3.A		–0.5	
1-cell	3.B	1	0	The blastodisc consists of one cell
<b>Cleavage period</b>				
2-cell	3.C	1	0.5	2 blastomeres
4-cell	3.D	1	1	2 X 2 array of blastomeres
8-cell	3.E	1	1.5	2 X 4 array of blastomeres
16-cell	3.F	1	2	4 X 4 array of blastomeres
32-cell	3.G	1	2.5	2 X 8 array of blastomeres
64-cell	3.H	1	3	Blastodisc consists of two layers of cells
<b>Blastula period</b>				
seventh cleavage	4.A	1	3.5	High mound of cells
eighth cleavage	4.B	1	4	High mound of cells
High-cell stage	4.C	1	5.5	High mound of cells
Sphere	4.D	1	6.5	Interface between the blastodisc and the yolk nearly flat, resulting in a hemispherical shape of the blastodisc
Dome	4.E	1	9	Shape of the blastula remains spherical; yolk bulging toward animal pole
30% epiboly	4.F	1	9.5	Blastoderm is of uniform thickness and starts to cover the yolk
<b>Gastrula period</b>				
Germ-ring	5.A	1	10.5	Germ-ring is visible
Shield	5.B	1	12.5	Embryonic shield is visible
50% epiboly	5.C	1–2	15	Embryonic axis is formed
75% epiboly	5.D	2	17.5	Head primordium, brain rudiment and tail bud are visible
90% epiboly	5.E	2	19	Formation of the yolk plug
100% epiboly	5.F & 5.G	2–3	21	Kupffer's vesicle forms as well as 3 somite furrows
<b>Segmentation period</b>				
6-somite	6.A	3	23	Rudiment of the brain subdivides- optic primordia is formed
12-somite	6.B	3	27.5	Melanophore appear over the yolk
15-somite	6.C	3	29.5	Notochord, lens primordium, rudiment of cerebellum and ephiphysis are visible
18-somite	6.D	3	32.5	The otic vesicle starts to form
22-somite	6.E	3	34.5	v-shaped trunk somites and twitching of the trunk muscles are observed
<b>Organogenesis period</b>				
25%-OCV	7.B	4	44	Orientation of embryo changes within the chorion. Pericardial cavity formed
40%-OCV	7.C	4	55	Eyes start to show black pigmentation. The heart and medial fin fold form
80%-OCV	7.D	4	75	Vascularization of the yolk, formation of the cardinal vein
4 dpf	7.E	none	4 dpf	Orange xanthophores appear, pectoral fin and cloaca are visible
5 dpf	7.F	none	5 dpf	Heart moves anteriorly, the mouth opens, formation of opercules
6 dpf	7.G	none	6 dpf	Eyes are silver, lower jaw extends anteriorly and becomes vascularized
7 dpf	7.H	none	7 dpf	Gills are visible and the jaw becomes thicker

## 2.4 | Blastula period

The blastula period extends from the seventh set of cleavages until gastrulation. Cleavages occur with increasing

irregularity. The blastodisc acquires a more uniform appearance, and starts to thin and spread around the yolk (epiboly). When 30% of the yolk is covered by the blastodisc, gastrulation begins (Figure 4- Movie 1).

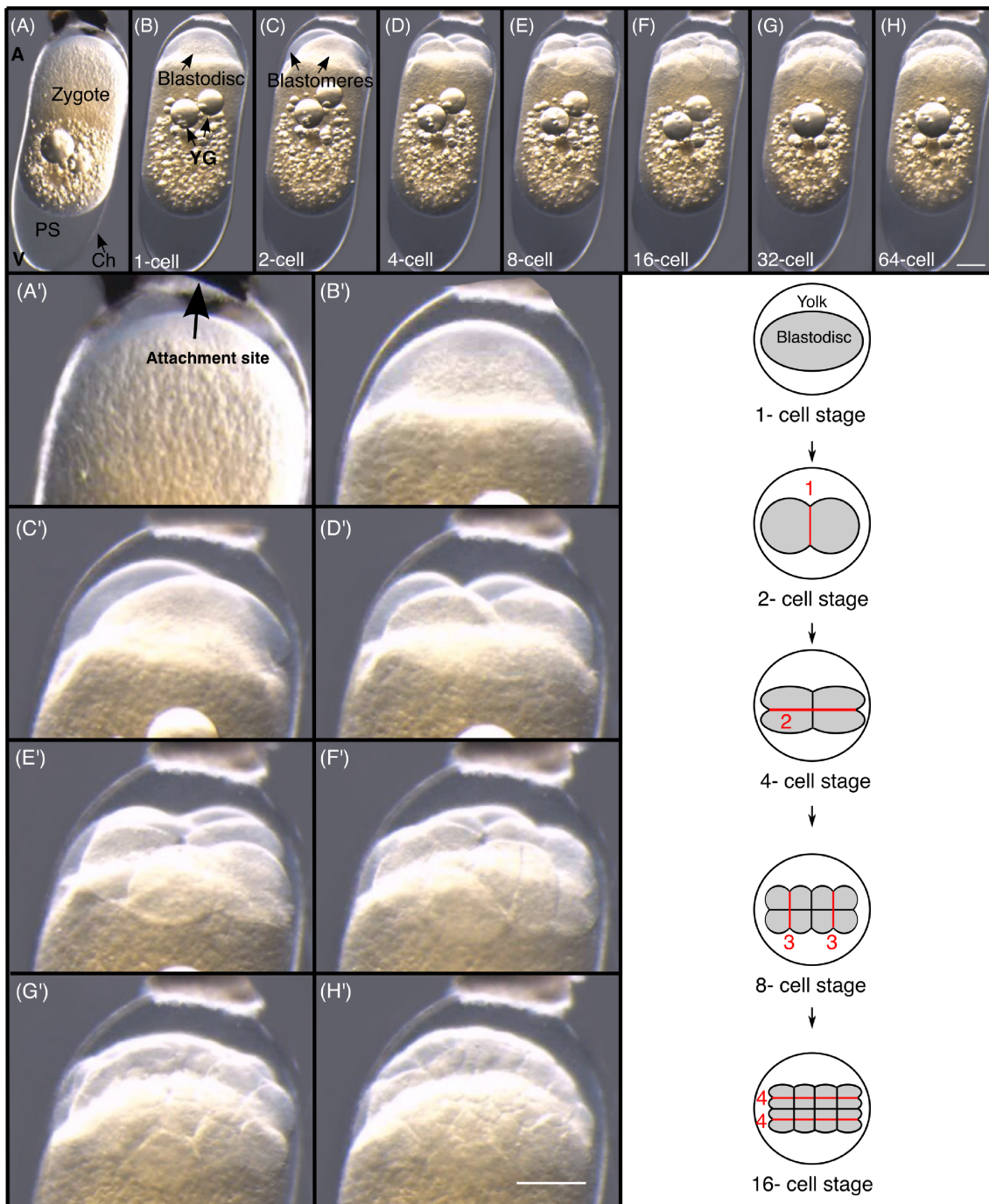


**FIGURE 3** Zygotic and cleavage periods. Lateral view of embryos at zygotic (A, A', B, B') and cleavage periods (C to H and C' to H'). The zygote is formed of the yolk sac and the blastula which is located at the animal pole of the adhesive egg (B to H and B' to H'). The cleavage period is divided into 6 stages: (C and C') 2-cell stage, (D and D') 4-cell stage, (E and E') 8-cell stage, (F and F') 16 cell stage, (G and G') 32-cell stage and (H and H') 64-cell stage. (I) Cartoon representing a dorsal view of embryos during cleavage period. The planes of divisions from 1-cell to 16-cell stage are in red lines. Scale bar = 200  $\mu\text{m}$ . A, Animal pole; Ch, chorion; PS, perivitelline space; V, vegetative pole; YG, yolk globule

**High-cell stages (3.5 hpf to 5.5 hpf):** Cleavages continue to occur; however, no clear cleavage planes can be identified. The seventh cleavage stage (3.5 hpf—Figures 4A and A'), eighth cleavage stage (4 hpf—Figures 4B and B') and high-cell stages (5.5 hpf—

Figures 4C and C') result in blastomeres that become smaller, without a clear increase in the size of the blastodisc (Figures 4A–C, Movie 1).

**Sphere-stage (6.5 hpf):** After the high-cell stage, the interface between the lower part of the blastodisc and



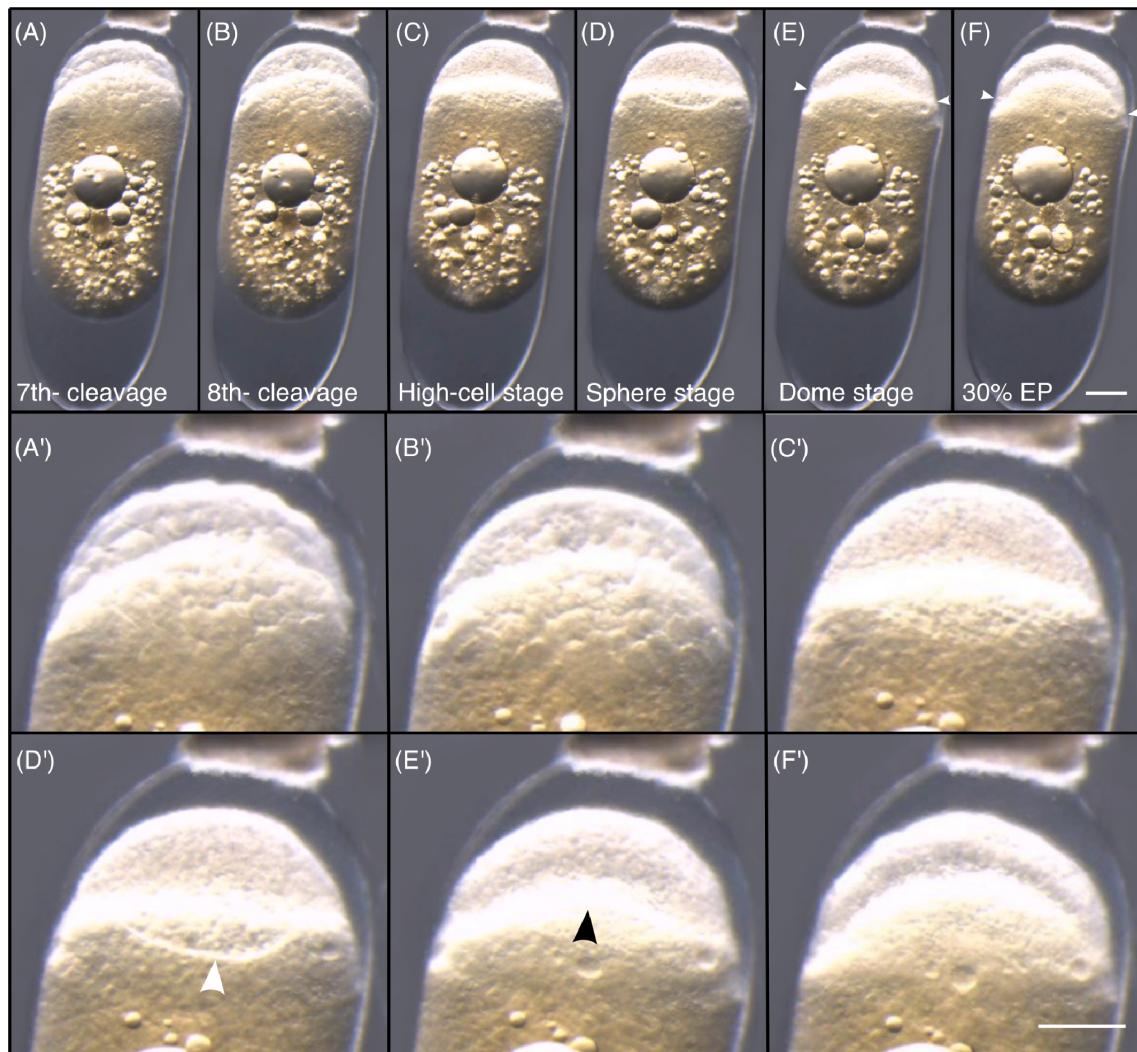


**FIGURE 4** Blastula period. (A-F and the corresponding magnification A'-F') Stereomicroscope images of the six stages during blastula period: (A, A') seventh cleavage stage; (B, B') eighth cleavage stage; (C, C') high-cell stage. (D, D') At sphere stage, the limit between the upper part of the yolk and the blastodisc is becoming conspicuous (white arrowhead). (E, E') At dome stage, deep in the blastodisc, the yolk begins to dome toward the animal pole (black arrowhead). (F, F') 30%-Epiboly stage. White arrowheads in E and F point to the edge of the blastoderm to better visualize epiboly's progression. Scale bar = 200  $\mu$ m

the upper part of the yolk is flat or nearly flat, resulting in a hemispherical shape of the blastodisc (Figures 4D and D'). We can distinguish the sphere-stage from the high-cell stage by the limit between the upper part of the yolk and the blastodisc that is becoming conspicuous (white arrowhead, Figure 4D'-Movie 1), which seems to result from a uniform increase in pressure against the yolk.

**Dome-stage (9 hpf):** The flattening of the blastodisc continues (Figures 4E and E'), starting to cover the top of the yolk, which bulges towards the animal pole in a dome-like shape (black arrowhead, Figure 4E').

**30% epiboly stage (9.5 hpf):** The blastodisc, which gradually transforms into a uniformly thick layer, starts to cover the yolk and is now called the blastoderm. This

stage can be measured by the percentage of epiboly, specifically the ratio of the distance from the animal pole to the blastoderm margin and the distance from the animal to the vegetal pole of the embryo (Figures 4F and F').

## 2.5 | Gastrula period

Gastrulation is defined as the period during which cellular movements (involution, convergence and extension) of the blastoderm tend to form the embryonic axis and the organization of the germ cell layers: the epiblast that will give rise to a part of the ectoderm, the hypoblast that corresponds to the future mesoderm and endoderm.<sup>32</sup>



When 30% epiboly is reached, the germ-ring forms and the embryonic shield is visible at the dorsal side of the blastoderm margin. Gastrulation starts at 30% epiboly in *A ocellaris* and epiboly continues until the blastoderm completely covers the yolk, with a speed of epiboly of about 9.5% per hour. The gastrula period is differentially divided into 6 stages: Germ-ring stage, shield stage, 50%-epiboly, 75%-epiboly, 90%-epiboly, and 100%-epiboly (Figure 5-Movies 1 and 2).

**Germ-ring stage (10.5 hpf):** The percent-epiboly is almost the same as at the 30%-epiboly stage. The germ-ring can be observed as a stripe at the most vegetal pole-side of the blastoderm margin along the equatorial plane (Figures 5 A, A'- Movie 1).

**Shield stage (12.5 hpf):** A thickening appears at one position of the blastoderm margin (now defined as the dorsal side) (Figures 5B, B'-Movie 1). This thickening is

referred to as the “embryonic shield” and is the result of cellular movements.<sup>32</sup> Gastrulation and cell involution take place in this part of the blastoderm.<sup>32</sup>

**50%-epiboly stage (15 hpf):** Epiboly moves the blastoderm margin to 50% of the distance between the animal and vegetal pole (Figures 5 C, C'-Movies 1 and 2). At this stage, the dorsal side of the blastoderm thickens further and the future embryonic axis becomes visible, with the anterior end in the direction of the animal pole.

**75%-Epiboly (17.5 hpf):** Epiboly displaces the blastoderm margin to 75% between the ends of the animal and vegetal poles (Figures 5 D, D'- Movie 2). At this stage, the head primordium develops anteriorly and the brain rudiment is visible. The posterior end of the embryonic axis develops a distinct swelling, the tail bud.

**90%-Epiboly (19 hpf):** The remnant of uncovered yolk protruding from the neighborhood of the vegetal pole

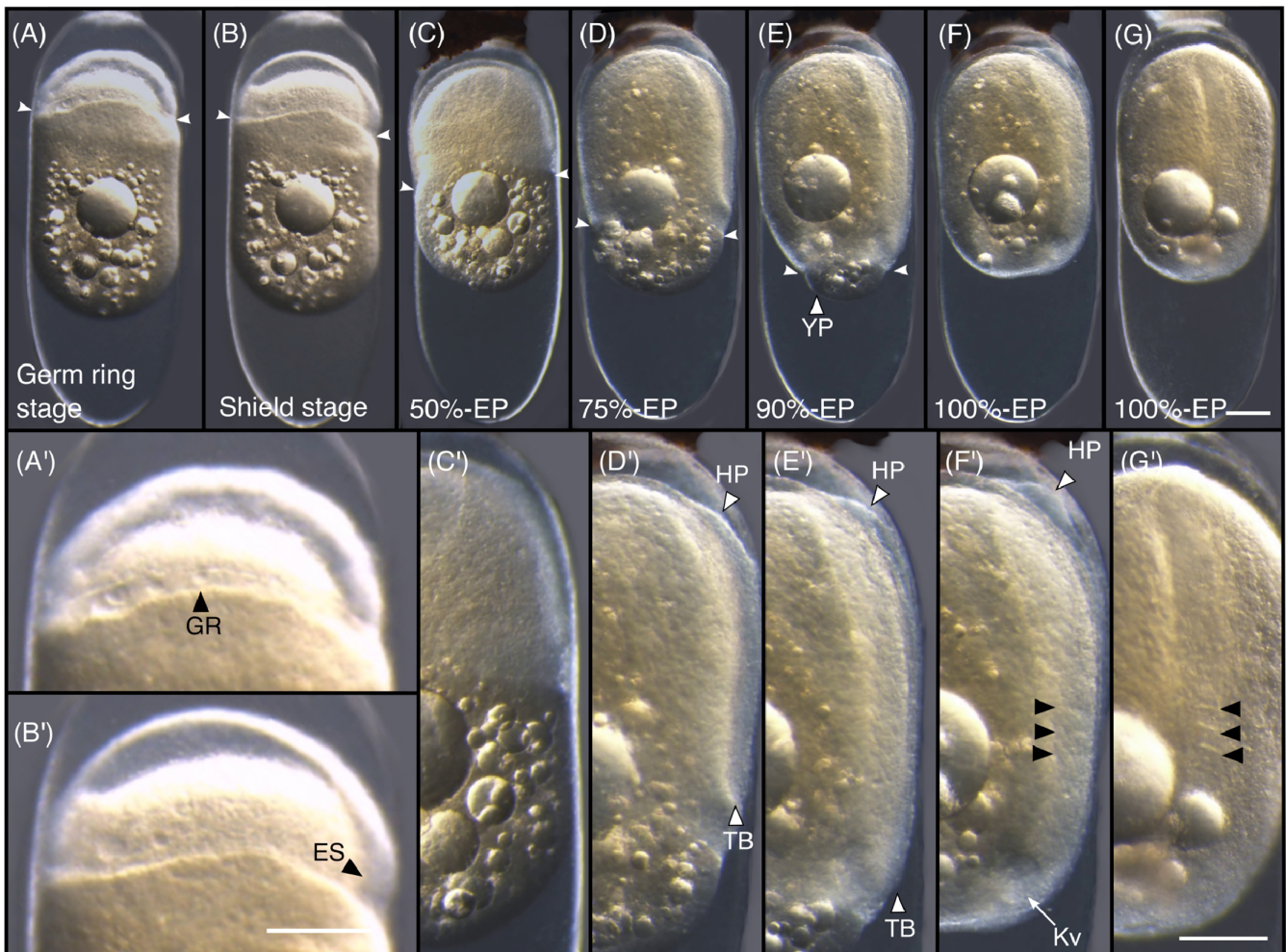


**FIGURE 5** Gastrula period. (A-F and the corresponding magnification A'-F') Lateral and (G-G') dorsal stereomicroscope images of embryos at each stage of gastrula period: (A-A') germ-ring stage, (B-B') shield stage, (C-C') 50%-epiboly stage, (D-D') 75%-epiboly stage, (E-E') 90%-epiboly stage, (F-F' and G-G') 100%-epiboly stage. Black arrowheads in F' and G' show somite furrow. White arrowheads (A to E) point to the edge of the blastoderm to better visualize epiboly's progression. ES, embryonic shield; GR, germ ring; HP, head primordium; Kv, Kupffer's vesicle; TB, tail bud; YP, yolk plug. Scale bar = 200  $\mu$ m

may be now considered a yolk plug, the section of the yolk at the vegetal pole that has not been covered by the blastoderm (Figures 5 E, E'-Movie 2).

**100%-Epiboly stage (21 hpf):** Epiboly ends as the blastoderm completely covers the yolk plug, defining 100%-epiboly. The Kupffer's vesicle forms (Figure 5F') and the first three somites are visible. (Figures 5 F, F', G, G'-Movies 2 and 3).

## 2.6 | Segmentation period

The long axis of the embryo starts to extend even before epiboly is complete, and continues to do so during the segmentation period. Structures including the somites, tail, eyes and auditory vesicles begin to form. Additionally, the brain subdivisions start to become visible, and pigmentation appears, first on the yolk sac and later on

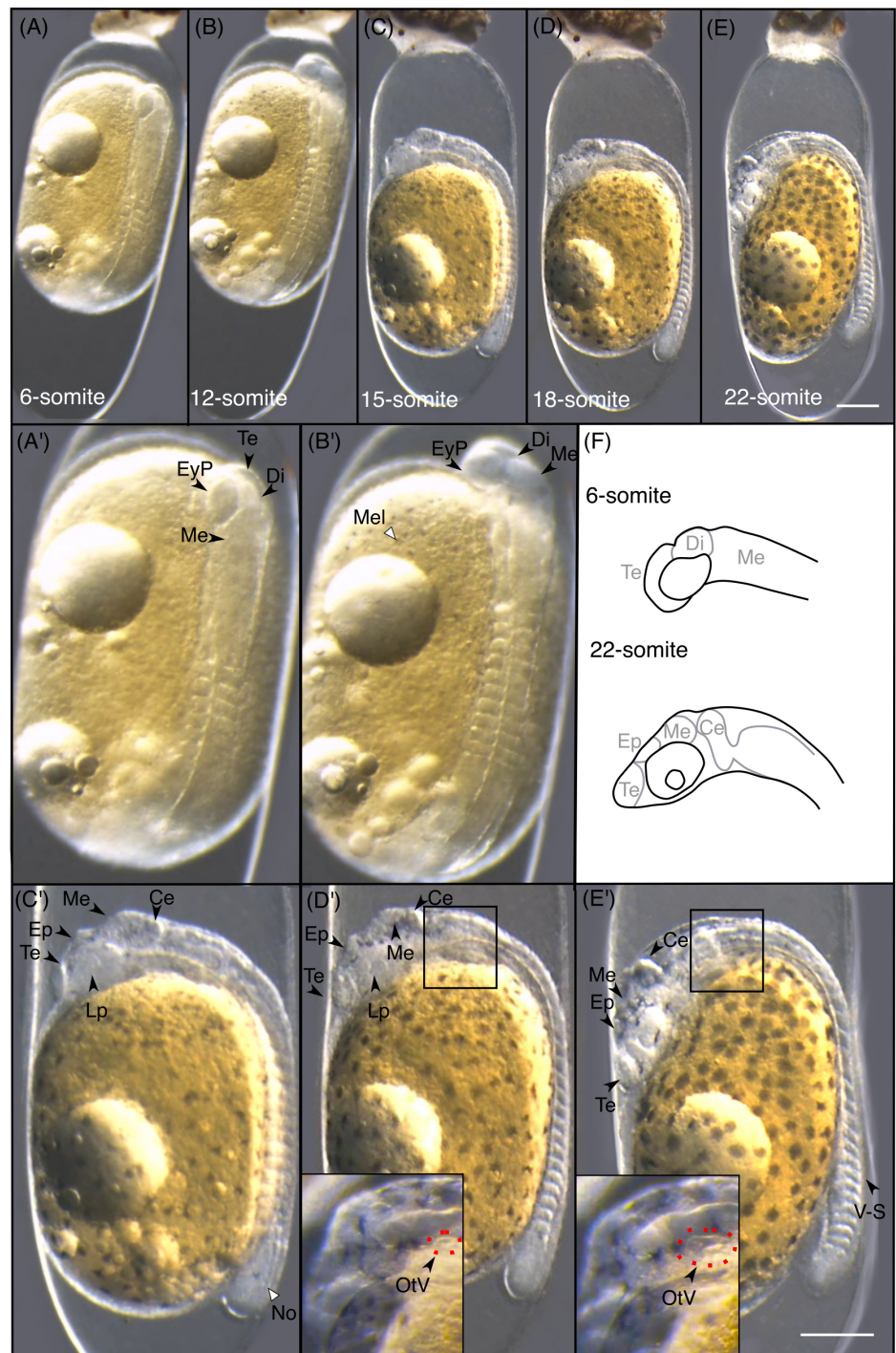


**FIGURE 6** Segmentation period. (A-E and the corresponding magnification A'-E')

Stereomicroscope images of embryos at all stages of segmentation period: (A-A') 6-somite stage, (B-B') 12-somite stage, (C-C') 15-somite stage, (D-D') 18-somite stage and (E-E') 22-somite stage. (F) Cartoon showing the development of the brain between 6 and 22-somite stages. Ce, cerebellum; Di, Diencephalon; Ep, epiphysis; EyP, eye primordium; Me, metencephalon; Mel, melanophore; No, notochord; Lp, lens primordium; OtV, otic vesicle; Te, telencephalon; V-S, V-shaped somites. Scale bar = 200 μm



the body axis (Figure 6-Movie 3). From the 1- to 18-somite stage, the rate of somite appearance is approximately one somite every 35 min.

Using somite number, we categorize the segmentation period of false clownfish embryos. Because false clownfish embryos at the late gastrula stage already possess three somites, the gastrula stage and segmentation period overlap slightly.

**6-somite stage (23 hpf):** The epiboly is complete (100%-epiboly) (Figures 6 A, A'-Movie 3). Six somites have formed and the tail bud is prominent at the posterior end of the body axis. At the anterior end of the embryo, the rudiment of the brain begins to subdivide and we can distinguish the telencephalon, the diencephalon and the mesencephalon (Figure 6F). The optic primordium (or eye primordium) is formed.

**12-somite stage (28.5 hpf):** At the 12-somite stage, the first melanophores are visible on the yolk (Figures 6B, B'-Movie 3).

**15-somite stage (30.5 hpf):** The notochord is clearly visible (Figures 6C, C'-Movie 3). At the posterior end, the tail bud begins to separate from the body as it becomes more elongated (Figure 6C, C'-Movie 3). At the anterior end, the lens primordium starts to be visible as well as the rudiment of the cerebellum and epiphysis (Figure 6C, C', F-Movie 3).

**18-somite stage (32.5 hpf):** The otic vesicle starts to form (Figure 6D, D'-Movie 3).

**22-somite stage (34.5 hpf):** This stage is characterized by the formation of V-shaped trunk somites (Figure 6E, E'). The twitching of the trunk muscles can also be observed (Movie 3).

## 2.7 | Organogenesis

From the late segmentation stage onward, the embryo starts to turn itself within the chorion (Movie 4). Organogenesis starts when the embryo has a well-developed notochord, the brain is highly sculptured, and the lens primordia and otic vesicles are visible. The following changes then occur: the tail (post-cloacal region) begins to elongate and the heart, the median fin fold (ventral and dorsal) and the pectoral fins form. At the same time, larval pigmentation starts to form: the pigmented retinal epithelium becomes prominent and the melanophores begin to arrange themselves in a characteristic pattern that includes a well-defined set of longitudinal body stripes.

To stage the embryos at the beginning of this period, we examine the "otic vesicle closure" (OVC), the ratio between the otic vesicle length and the distance between the otic vesicle and the eye border (Figure 7A). OVC increases at approximately 2% per hour during the organogenesis period (Figure 7A).

**25%-OVC (44 hpf):** At around 44 hpf, the embryo rotates in the chorion so that the tail is located close to the chorion's attachment site. The tail detaches from the yolk and is totally free within the chorion (Figure 7B). The pericardial cavity is visible. The median fin fold is not yet formed.

**40%-OVC (55 hpf):** At 40%-OVC (Figure 7C), the black pigmentation of the eye starts and a well-formed heart is visible. The median fin fold is now formed at the dorsal and ventral side of the posterior area.

**80%-OVC (75 hpf):** At 80%-OVC, blood cells occupy the yolk (Figure 7D-stars) over very ill-defined and broad regions that herald the development of the common cardinal vein (Figure 7D- white arrowheads). The eyes' black pigmentation is more prominent.

At 4 dpf, the embryo reaches 85-90%-OVC and after this stage there is no clear quantitative or presence/absence feature that allows for the definition of unambiguous stages. For the last days of development, we therefore present one picture per day of the embryo with (Figure 7E-H) and without the chorion (Figure 7E'-H'') and we briefly describe below the main differences existing between these fishes. The last 3 days of development are characterized by the formation of pectoral paired fins and craniofacial skeleton.

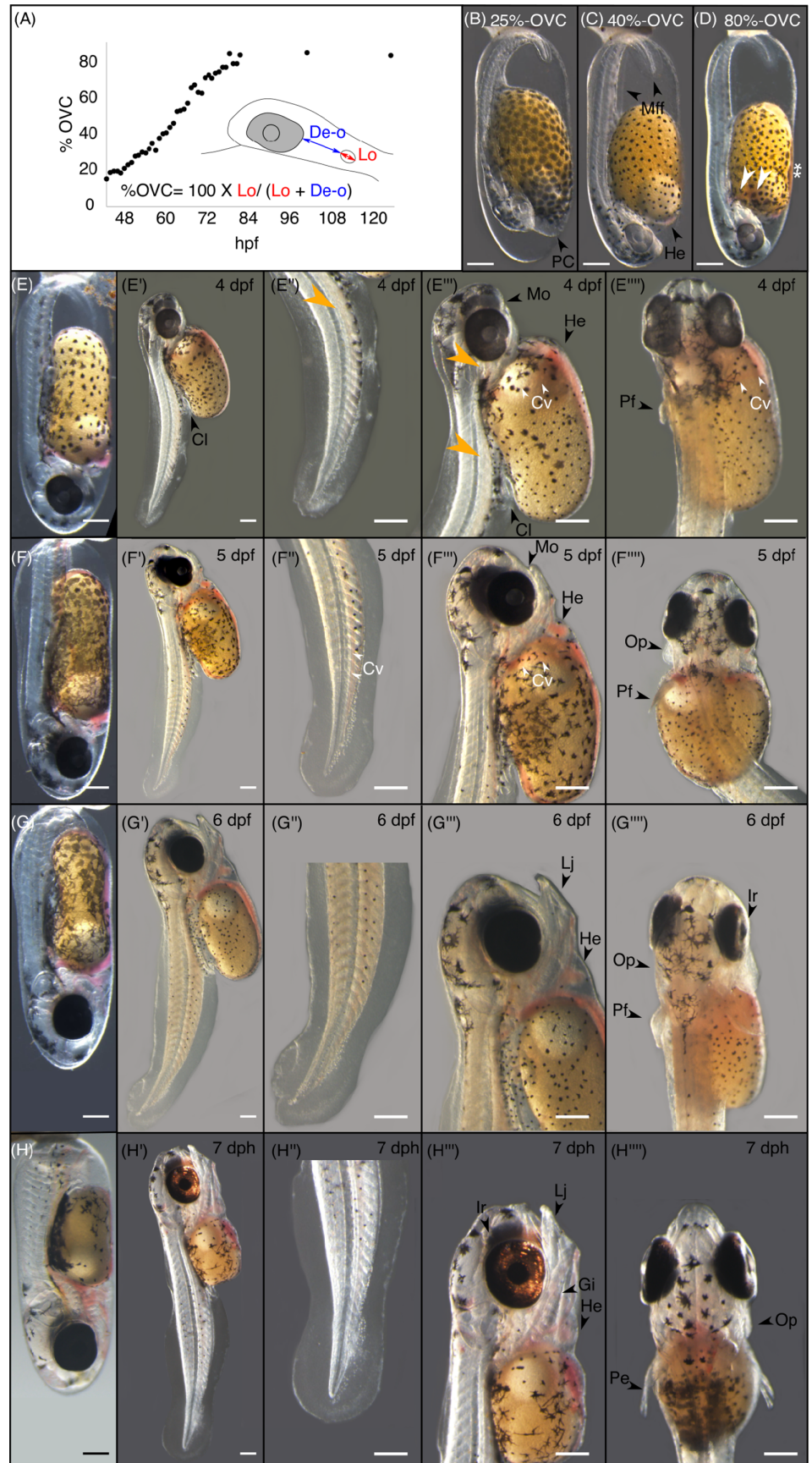
**4 dpf:** At 4 dpf (Figure 7E to E'''), a few pale orange xanthophores form on the ventral side of the trunk and posterior to the eye (Figure 7E'''- orange arrowheads). The common cardinal vein can be recognized as a pink tube in the lateral view (Figure 7E''' and E'''-white arrowheads). From this stage onward, the pectoral fin is elongated posteriorly (Figure 7EE'''). The posterior part of the median fin fold (ventral and dorsal) is enlarged (Figure 7E'''). The cloaca is formed and the mouth opens antero-ventrally (Figure 7E''').

**5 dpf:** The posterior part of the median fin (ventral and dorsal) begins to expand in a dorsoventral direction. The cardinal vein extends to the posterior region (Figure 7F''). At this stage (Figures 7F-F'''), the pectoral fin elongates posteriorly. The lens' black pigmentation increases. The position of the heart is visibly different between previous stages and this stage; the heart moves to the anterior, and is located at the anterior aspect of the yolk at this stage. Mouth openings are more anterior than at 4 dpf. The opercula can be observed in the ventral cranial region (Figure 7F''').

**6 dpf:** The embryo further increases in size (Figure 7G to G'''). The eyes become silver. The lower jaw extends anteriorly, elongating the head in a more anterior direction. The jaw becomes vascularized.

**7 dpf:** Melanophores form two horizontal stripes on the tail and concentrate ventrally just dorsal to the yolk (Figure 7H to H'''). Gills are clearly visible.

**FIGURE 7** Organogenesis period. (A) Cartoon representing the “Otic vesicle closure” index (OVC). OVC corresponds to the ratio between the otic vesicle length (Lo) and the distance between the otic vesicle and the eye border (De-o + Lo). Graph represents the %-OVC from 40 hpf until 5 dpf. Stereomicroscope images of embryos during organogenesis period: (B) 25%-OVC, (C) At 40%-OVC, (D) 80%-OVC, (E, E', E'', E''', E''''') 4 dpf; (F, F', F'', F''', F''''') 5 dpf, (G, G', G'', G''', G''''') 6 dpf, and (H, H', H'', H''', H''''') 7 dpf. Formation of blood circulation is indicated with white stars and arrowheads. Orange arrowheads point to orange xanthophores. Cl, cloacal; Cv, cardinal vein; Gi, gills; He, heart; Ir, iridophores; Lj, Lower jaw; Mff, median fin fold; Mo, mouth; Op, opercula; PC, Pericardial cavity; Pf, pectoral fin. Scale bar = 200  $\mu$ m



## 2.8 | Hatching

False clownfish embryos hatch generally once the lights are off 7 days after fertilization at 26°C (in our conditions). However, in some clutches we observed a one-day delay between one part of the clutch and the other.

The embryo hatches by breaking the egg capsule with its active wriggling, and the hatchlings emerge tail first (Figure 8A to A"). Because hatching was first observed in eggs that were scraped off of the terracotta pot, we wondered how hatching occurs when eggs are still fixed to their substrate. We succeeded in directly observing this event and the hatching sequence was the same (Figure 8B). Larvae in eggs which have been detached from their substrate may have difficulty extracting themselves from the chorion, but this is of course not the case with attached eggs. Once hatching occurs, young larvae still have some yolk (Figure 8C) and are immediately capable of swimming (data not shown).

## 2.9 | The development of larval pigmentation pattern

As the development of pigmentation is prominent during the embryonic development of *A ocellaris*, particularly in the later stages, we thought it is important to summarize the different stages of the emergence of the larval pattern. Here, we describe development of two types of chromatophores, melanophores and xanthophores. We do not describe iridophore development because they are absent or not visible under the stereomicroscope, except those in the eye.

### 2.9.1 | Melanophores

Pigmentation by the melanophores is first observed from stage 12-somites (28 hpf) over the yolk; the melanophores migrate from the dorsal side of the yolk to reach the ventral side (29,5 hpf) (Figure 9A–D). Melanophores appear in the head region (Figure 9E) at 30 hpf, first localizing close around and behind the eyes (Figure 9E–H). On the trunk, pigmented melanophores appear in the posterior trunk between the embryo and the yolk (Figure 9G and H). Between 40 hpf and 7 dpf, the overall melanophore pattern does not change. At 7 dpf, tail melanophores localize along the myosepta to form a stripe, and ventral melanophores concentrate between the yolk and the ventral side of the embryo (Figure 9K).

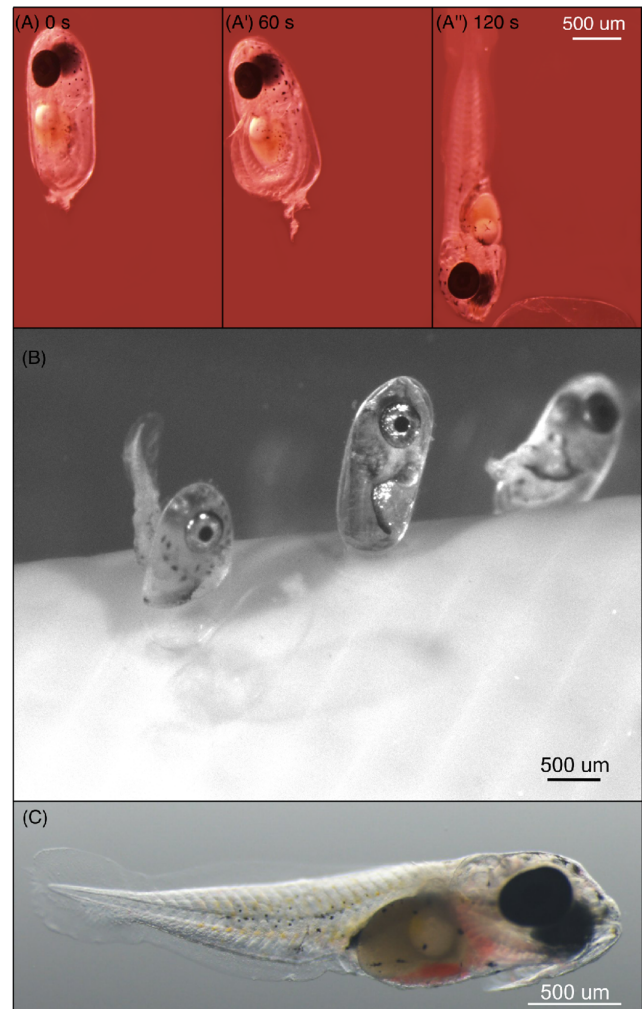


**FIGURE 8** Hatching. Time lapse of a 7dpf embryo hatching from a scraped egg (A–A") and when the egg is still attached to its substrate (B). (C) Stereomicroscope image of a young hatched larvae. Scale bar = 500  $\mu$ m

### 2.9.2 | Xanthophores

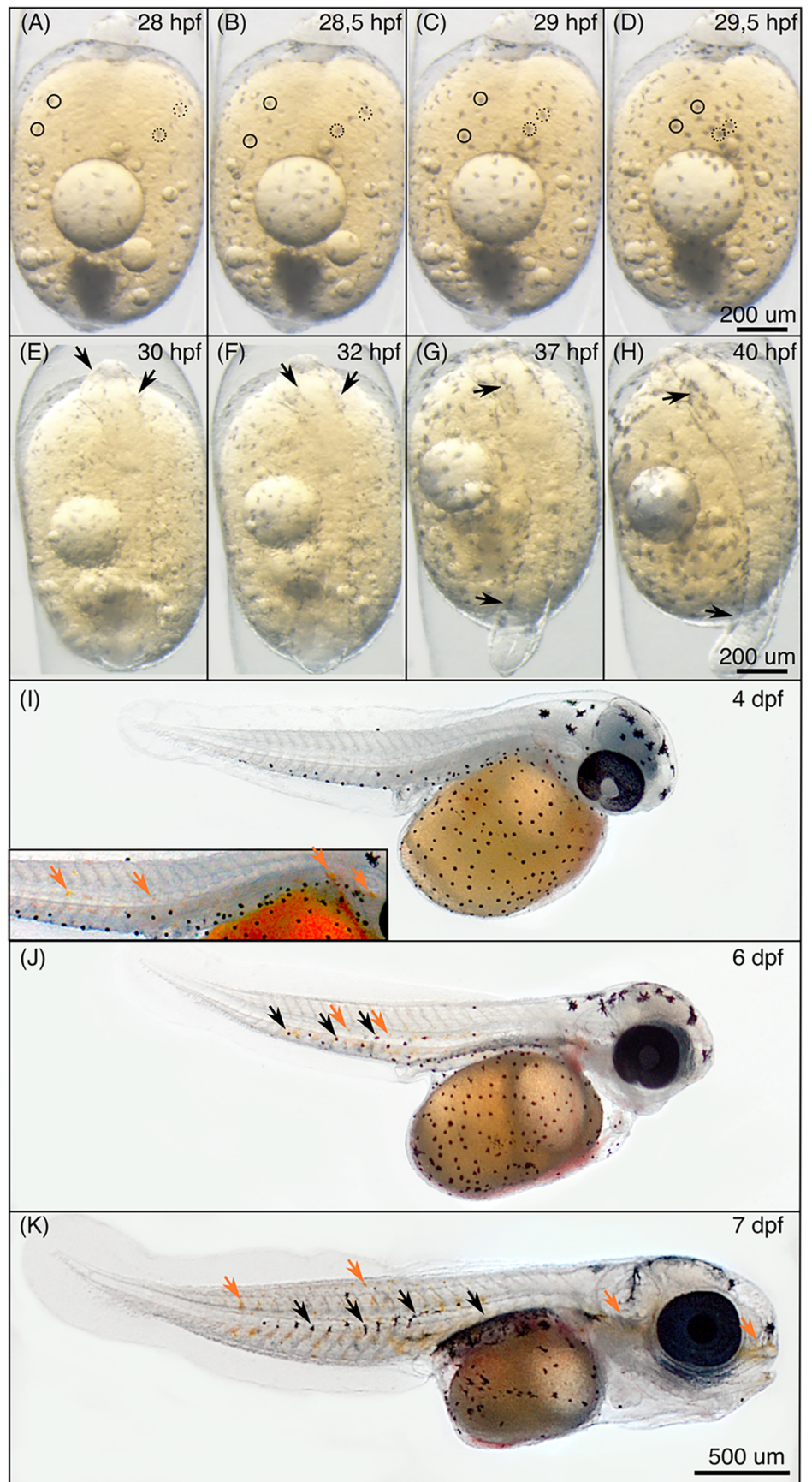
At 4 dpf, a few pale orange xanthophores form on the ventral side of the trunk and posterior to the eye (Figure 9I–crop). At 6 dpf, the dorsal side of the larvae is pigmented by xanthophores (Figure 9J). At 7 dpf, xanthophores form a stripe on the head that runs through the eye (Figure 9K).

## 3 | DISCUSSION

In this study, we provide a staging series organized similarly to other models such as zebrafish, goldfish, sea bass and Atlantic salmon<sup>14,32,34,35</sup> allowing for comparative studies. We also document the emergence of the larval



**FIGURE 9** Pigmentation throughout larval development. (A, B, C, D) Time-lapse pictures of a ventral view of a single embryo from 28 hpf to 29.5 hpf. Black circles follow single melanophores migration over the yolk. (E, F, G, H) Time-lapse pictures of dorsal view of an embryo. (I, J, K) Pictures of dechorionated embryos at 4 dpf (I and its associated focus), 6 dpf (J) and 7 dpf (K). Black and orange arrows point respectively to melanophores and xanthophores



pigmentation pattern that we have recently provided,<sup>33</sup> linking embryonic development with the conspicuous adult pigmentation pattern of this species. These data provide a general framework that can be used as a tool to standardize studies and experimental procedures throughout false clownfish development.

### 3.1 | False clownfish embryonic development in the teleost fishes context

Similar to previous studies on teleost development, we describe six periods of embryogenesis during embryonic development of *A ocellaris*, namely the zygote, cleavage, blastula, gastrula, segmentation, and organogenesis periods, as well as 32 stages (Table 1 and Figure 2) reminiscent of those described in other models such as zebrafish, medaka, cichlids, and goldfish.<sup>11,14,32,36</sup> These well-defined stages provide a framework for testing hypotheses of homologies within the various processes that occur during the embryonic development of teleost fishes. We observed interesting morphological differences between the embryos of false clownfish and other teleost species, whether they are aquaculture species (the sea bass *Dicentrarchus labrax*,<sup>34</sup> the turbot *Scophthalmus maximus*,<sup>37</sup> the batfish *Platax teira*<sup>38</sup>), other coral reef fish (the damselfish *Neopomacentrus cyanomus*,<sup>19</sup> the dottedbacks *Pseudochromis dilecticus*,<sup>17</sup> the mandarin fish *Synchiropus splendidus*,<sup>39</sup> the goby *Elacatinus puncticulatus*,<sup>40</sup> several angelfishes of the genus *Centropyge*<sup>18,41</sup>) or other fish models (the stickleback *G aculeatus*, the salmonid *Coregonus clupeaformis*,<sup>12</sup> the gadid *Trisopterus luscus*,<sup>42</sup> the wrasse *Labrus bergylta*<sup>43</sup>). These include the shape of the yolk/chorion, different early chromatophore patterns, and variation in developmental timing. Because of its specific life history traits (fixed eggs from a benthic marine fish, relatively long embryonic development with an immediately active larvae and a short pelagic larval duration or PLD), the false clownfish differs from most of the models for which embryonic development has been recently described with precision (see<sup>20</sup> and references therein).

By comparing the growth and development of the larvae of four damselfish including an anemonefish (*Premnas biaculeatus*), Kavanagh and Alford, 2003 found a highly significant negative correlation between the duration of embryonic development and PLD that was also observed when more species were taken into account.<sup>44,45</sup> This is not surprising, as damselfish life history strategies vary widely,<sup>45</sup> and a shift in one life history trait can trigger the coordinated evolution of many other traits (eg, imprinting on sea anemone odor at hatching might require earlier development of the olfactory

system<sup>46</sup>). Changing the respective duration of embryonic development and settlement time or altering with growth and developmental rates constitutes the range of levels on which evolution can operate to ensure the best possible survival in a vast series of ecological possibilities. This flexibility undoubtedly explains the great success of damselfishes and, this has yet to be demonstrated in other teleost fishes clades. The link between egg size, duration of embryonic development and short PLD, three features that differ between most other coral reef fishes, will be very interesting to study in more detail.<sup>44,47</sup>

### 3.2 | The emergence of the larval pigmentation pattern

False clownfishes are well known for their iconic pigmentation patterns with three white bars formed by iridophores, lined with black melanophores on an orange background of xanthophores.<sup>48,49</sup> This pattern emerges during metamorphosis, differs from the simpler larval pattern, and appears to be formed differently than the pattern of horizontal stripes well-studied in zebrafish.<sup>50,51</sup>

The emergence of pigmentation during embryonic development occurs in three main steps (i) it starts by the appearance of melanophores over the yolk at the 12-somites stages (28 hpf). These cells then migrate toward and invade the entire yolk at 30 hpf (Figure 9 A-D). (ii) At 30 hpf, melanophores appear in the vicinity of the eyes (Figure 9E) and later on the tail and in the posterior trunk at the border with the yolk (Figure 9F-H). Around 4dpf pale orange xanthophores are visible on the ventral side of the trunk and posterior to the eye (Figure 9I) (iii) Lastly, at 7 dpf, some melanophores localize along the myosepta to form a stripe and ventrally concentrate at the border between the yolk and the ventral side of the embryo (Figure 9K). At that stage xanthophores form a stripe that runs through the eye (Figure 9K). Interestingly, this pattern seems to be very similar between all anemonefishes, including *P biaculeatus* and *Amphiprion perideraion*, in which lateral black marks of melanophores over a yellow pale body are clearly visible at hatching.<sup>52,53</sup>

The embryonic melanophore pattern that we observe in *A ocellaris* is very different from those described in other teleost models such as cichlid fishes, medaka and zebrafish. Zebrafish, at hatching, have two dorsal and lateral melanophore stripes that originate from waves of migrating neural crest cells.<sup>51</sup> In *A ocellaris* these larval stripes are not present, suggesting a different migration pattern of neural crest cells,<sup>51</sup> which are thought to generate all but the yolk melanophores in teleosts.<sup>51,54</sup> In cichlids a single prominent ventral stripe of melanophores is visible.<sup>11</sup> Further analysis using neural crest

markers could clarify the difference in ontogenetic processes that causes the emergence of such different melanophore patterns in teleosts. The genetic dissection of the diversity of this early and relatively simple pattern can be a relevant model to study the molecular and developmental basis of trait diversity.

## 4 | CONCLUSIONS

In this study, we provide a detailed illustrated and filmed embryonic developmental table for a coral reef fish: the false clownfish *A ocellaris*. It is our hope that this staging will facilitate work with *A ocellaris* as a model species, which can be used to better understand the genesis of coral reef fish developmental trajectories and how they are impacted by environmental perturbations.<sup>55</sup> This emerging model will also allow investigation of a wide variety of biological questions such as the control of behavior, the diversification of pigmentation patterns and the link between embryonic development and life history strategies.<sup>20</sup>

## 5 | EXPERIMENTAL PROCEDURES

### 5.1 | *A ocellaris* rearing conditions

*A ocellaris* used for imaging were obtained from different clutches laid by a single *A ocellaris* breeding pair at the ICOB Marine Research Station in Taiwan, but the timing of events presented here aligns with that of the embryos of other pairs raised in Observatoire de Banyuls-Sur-Mer, France. The breeding pair was held in a 120-L tank of natural sea water at a temperature of 26°C, and a 12:12 h light: dark photoperiod.<sup>56</sup> Adult fish were fed twice daily with live food including shrimp, squid, and the Japanese scad *Decapterus maruadsi*. Egg clutches were laid on a terra-cotta pot in the breeding tank.

### 5.2 | Stereomicroscope acquisition of high-resolution images and videos of *A ocellaris* embryonic development

To follow the developmental changes occurring during embryonic development, we performed time-lapse using brightfield transmitted illumination of at least three embryos. Larvae were placed in a drop of filtered sea water on a Petri dish under the stereomicroscope. Live images were acquired on stereomicroscope (OLYMPUS SZX16, 1XPF) using a camera (DP80 using software

CellSens DP80) with a picture resolution of 1360 x 1024 pixels and a time exposure of 142.9 ms (time-frame of 1 image/min). Measurements were performed using ImageJ software (V1.51k). For time-lapse of hatching, because embryos will not hatch under bright light, we placed a red plastic bag under the petri dish to decrease brightfield transmitted illumination.

## ACKNOWLEDGMENTS

We thank the aquariology service of the Yilan Marine Research Station (ICOB, Academia Sinica in Taiwan), who provided the larvae used in this study. We also deeply thank Kinya Ota who provided a great help for microscopy and time-lapse movie settings and acquisitions. We thank Carole Petetin who drew Figure 1. We also thank Stephanie Bertrand, Laurence Besseau, Marleen Klann, Jamie Canepa, and Billy Moore for their help on the morphological observations and critical reading of the manuscript. This study was supported by Agence Nationale de la Recherche (ANR-19-CE34-0006-Manini and ANR-19-CE14-0010-SENSO).

## CONFLICT OF INTEREST

The authors declare that they have no competing interests.

## ETHICS APPROVAL

These experiments were approved by the C2EA-36 Ethics Committee for Animal Experiment Languedoc-Roussillon (CEEA-LR), number A6601601. We have an approval number (A6601601) of premises for animal testing issued by the Regional Directorate of Food, Agriculture and Forestry of Occitania, and the Departmental Directorate of Protection of Populations of the Pyrenees Orientales. The animals were raised in our lab from breeding stock. Experimental protocols were based on the regulations in force in France (Articles R214-87 to R214-137 of the Rural Code), updated by Decree 2013-118 and by five decrees dated February 1, 2013, and published February 7, 2013, pursuant to Directive 2010/63/EU. This regulation is under the responsibility of the Ministry of Agriculture.

## ORCID

Pauline Salis  <https://orcid.org/0000-0002-5690-3714>

Natacha Roux  <https://orcid.org/0000-0002-1883-7728>

Vincent Laudet  <https://orcid.org/0000-0003-4022-4175>

## REFERENCES

1. Alfred J, Baldwin IT. New opportunities at the wild frontier. *Elife*. 2015;4:e06956.



2. Goldstein B, King N. The future of cell biology: emerging model organisms. *Trends Cell Biol.* 2016;26(11):818-824.
3. Patton EE, Zon LI. The art and design of genetic screens: zebrafish. *Nat Rev Genet.* 2001;2(12):956-966.
4. Takeda H, Shimada A. The art of Medaka genetics and genomics: what makes them so unique? *Annu Rev Genet.* 2010;44(1):217-241.
5. Nelson JS, Grande TC, Wilson MVH. *Fishes of the World.* John Wiley & Sons, Inc: Hoboken, NJ, USA; 2016.
6. Cresko WA, McGuigan KL, Phillips PC, Postlethwait JH. Studies of threespine stickleback developmental evolution: progress and promise. *Genetica.* 2006;129(1):105-126.
7. Jeffery WR. Emerging model systems in evo-devo: cavefish and microevolution of development. *Evol Dev.* 2008;10(3):265-272.
8. Martin KLM, Podrabsky JE. Hit pause: developmental arrest in annual killifishes and their close relatives. *Dev Dyn.* 2017;246(11):858-866.
9. Merilä J. Nine-spined stickleback (*Pungitius pungitius*): an emerging model for evolutionary biology research. *Ann N Y Acad Sci.* 2013;1289(1):18-35.
10. Travis J, Reznick D, Bassar RD, López-Sepulcre A, Ferriere R, Coulson T. Do eco-Evo feedbacks help us understand nature? Answers from studies of the Trinidadian guppy. *Adv Ecol Res.* 2014;50:1-40.
11. Kratochwil CF, Sefton MM, Meyer A. Embryonic and larval development in the Midas cichlid fish species flock (*Amphilophus spp.*): a new evo-devo model for the investigation of adaptive novelties and species differences. *BMC Dev Biol.* 2015;15(1):12.
12. Sreetharan S, Thome C, Mitz C, et al. Embryonic development of lake whitefish *Coregonus clupeaformis*: a staging series, analysis of growth and effects of fixation. *J Fish Biol.* 2015;87(3):539-558.
13. Swarup H. Stages in the development of the stickleback *Gasterosteus aculeatus* (L.). *J Embryol Exp Morphol.* 1958;6(3):373-383.
14. Tsai H, Chang M, Liu S, Abe G, Ota KG. Embryonic development of goldfish (*Carassius auratus*): a model for the study of evolutionary change in developmental mechanisms by artificial selection. *Dev Dyn.* 2013;242(11):1262-1283.
15. Cerdà J, Machado M. Advances in genomics for flatfish aquaculture. *Genes Nutr.* 2013;8(1):5-17.
16. Mazurais D, Darias M, Zambonino-Infante JL, Cahu CL. Transcriptomics for understanding marine fish larval development. *Can J Zool.* 2011;89(7):599-611.
17. Madhu K, Madhu R, Rethesh T. Spawning, embryonic development and larval culture of redhead dottyback *Pseudochromis dilatatus* (Lubbock, 1976) under captivity. *Aquaculture.* 2016;459:73-83.
18. Olivotto I, Holt SA, Carnevali O, Holt GJ. Spawning, early development, and first feeding in the lemonpeel angelfish *Centropyge flavissimus*. *Aquaculture.* 2006;253(1-4):270-278.
19. Setu SK, Ajithkumar TT. Spawning behaviour and embryonic development of regal damselfish, *Neopomacentrus cyanomus* (Bleeker, 1856). *World J Fish Mar Sci.* 2010;2(5):410-415.
20. Roux N, Salis P, Lee S-H, Besseau L, Laudet V. Anemonefish, a model for eco-Evo-devo. *Evodevo.* 2020;11(1):20.
21. Liew HJ, Ambak MA, Abol-Munafi AB. Embryonic development of clownfish *Amphiprion ocellaris* under laboratory conditions. *J Sustain Sci Manag.* 2006;1(1):64-73.
22. Yasir I, Qin JG. Embryology and early ontogeny of an anemonefish *Amphiprion ocellaris*. *J Mar Biol Assoc UK.* 2007;87(4):1025-1033.
23. Ghosh J, Wilson RW, Kudoh T. Normal development of the tomato clownfish *Amphiprion frenatus*: live imaging and in situ hybridization analyses of mesodermal and neurectodermal development. *J Fish Biol.* 2009;75(9):2287-2298.
24. Buston P. Size and growth modification in clownfish. *Nature.* 2003;424(6945):145-146.
25. Dixon DL, Jones GP, Munday PL, Planes S, Pratchett MS, Thorrold SR. Experimental evaluation of imprinting and the role innate preference plays in habitat selection in a coral reef fish. *Oecologia.* 2014;174(1):99-107.
26. Mitchell LJ, Valerio T, Marshall NJ, Cheney KL, Cortesi F. CRISPR/Cas9-mediated generation of biallelic G0 anemonefish (*Amphiprion ocellaris*) mutants. *bioRxiv.* 2020.
27. Quenouille B, Bermingham E, Planes S. Molecular systematics of the damselfishes (*Teleostei: Pomacentridae*): Bayesian phylogenetic analyses of mitochondrial and nuclear DNA sequences. *Mol Phylogenet Evol.* 2004;31(1):66-88.
28. Litsios G, Sims CA, Wüest RO, Pearman PB, Zimmermann NE, Salamin N. Mutualism with sea anemones triggered the adaptive radiation of clownfishes. *BMC Evol Biol.* 2012;12(1):212.
29. Marcionetti A, Rossier V, Roux N, Salis P, Laudet V, Salamin N. Insights into the genomics of clownfish adaptive radiation: genetic basis of the mutualism with sea anemones. Mank J, ed. *Genome Biol Evol.* 2019;11(3):869-882.
30. Schluter D. *The ecology of adaptive radiation.* Oxford: Oxford University Press; 2000.
31. Hopwood N. A history of normal plates, tables and stages in vertebrate embryology. *Int J Dev Biol.* 2007;51(1):1-26.
32. Kimmel CB, Ballard WW, Kimmel SR, Ullman B, Schilling TF. Stages of embryonic development of the zebrafish. *Dev Dyn.* 1995;203(3):253-310.
33. Roux N, Salis P, Lambert A, et al. Staging and normal table of postembryonic development of the clownfish (*Amphiprion ocellaris*). *Dev Dyn.* 2019;248(7):545-568.
34. Cucchi P, Sucré E, Santos R, Leclère J, Charmantier G, Castille R. Embryonic development of the sea bass *Dicentrarchus labrax*. *Helgol Mar Res.* 2012;66(2):199-209.
35. Gorodilov YN. Description of the early ontogeny of the Atlantic salmon, *Salmo salar*, with a novel system of interval (state) identification. *Environ Biol Fishes.* 1996;47(2):109-127.
36. Iwamatsu T. Stages of normal development in the medaka *Oryzias latipes*. *Mech Dev.* 2004;121(7-8):605-618.
37. Tong XH, Xu SH, Liu QH, Li J, Xiao ZZ, Ma DY. Stages of embryonic development and changes in enzyme activities in embryogenesis of turbot (*Scophthalmus maximus* L.). *Aquac Int.* 2013;21(1):129-142.
38. Leu M-Y, Tai K-Y, Meng P-J, Tang C-H, Wang P-H, Tew KS. Embryonic, larval and juvenile development of the longfin batfish, *Platax teira* (Forsskål, 1775) under controlled conditions with special regard to mitigate cannibalism for larviculture. *Aquaculture.* 2018;493:204-213.
39. Sadovy Y, Mitcheson G, Rasotto MB. Early development of the mandarin fish, *Synchiropus splendidus* (Callionymidae), with notes on its fishery and potential for culture. *Aquarium Sci Conserv.* 2001;3:253-263.

40. Pedrazzani AS, Pham NK, Lin J, Neto AO. Reproductive behavior, embryonic and early larval development of the red head goby *Elacatinus puncticulatus*. *Anim Reprod Sci*. 2014;145(1–2): 69–74.
41. Mendonça RC, Chen JY, Zeng C, Tsuzuki MY. Embryonic and early larval development of two marine angelfish, *Centropyge bicolor* and *Centropyge bispinosa*. *Zygote*. 2020;28(3):196–202.
42. Alonso-Fernández A, Vergara AR, Saborido-Rey F. Embryonic development and spawning pattern of *Trisopterus luscus* (Teleostei: Gadidae) under controlled conditions. *J Mar Biol Assoc UK*. 2011;91(6):1281–1287.
43. D'Arcy J, Dunaevskaya E, Treasurer JW, et al. Embryonic development in ballan wrasse *Labrus bergylta*. *J Fish Biol*. 2012; 81(3):1101–1110.
44. Kavanagh KD, Alford RA. Sensory and skeletal development and growth in relation to the duration of the embryonic and larval stages in damselfishes (Pomacentridae). *Biol J Linn Soc*. 2003;80(2):187–206.
45. Kavanagh K, Frédérick B. In: Frédérick B, Parmentier E, eds. *Biology of Damselfishes*. Boca Raton: Taylor & Francis; 2016 A CRC title: CRC Press; 2016.
46. Arvedlund M, Larsen K, Winsor H. The embryonic development of the olfactory system in *Amphiprion melanopus* (Perciformes: Pomacentridae) related to the host imprinting hypothesis. *J Mar Biol Assoc UK*. 2000;80(6):1103–1109.
47. Raff RA. *The shape of life: genes, development, and the evolution of animal form*. Vol 68. Chicago and London: University of Chicago Press; 1996.
48. Salis P, Roux N, Soulat O, Lecchini D, Laudet V, Frédérick B. Ontogenetic and phylogenetic simplification during white stripe evolution in clownfishes. *BMC Biol*. 2018;16(1):90.
49. Salis P, Lorin T, Lewis V, et al. Developmental and comparative transcriptomic identification of iridophore contribution to white barring in clownfish. *Pigment Cell Melanoma Res*. 2019; 32(3):391–402.
50. Salis P, Lorin T, Laudet V, Frédérick B. Magic traits in magic fish: understanding color pattern evolution using reef fish. *Trends Genet*. 2019;35(4):265–278.
51. Patterson LB, Parichy DM. Zebrafish pigment pattern formation: insights into the development and evolution of adult form. *Annu Rev Genet*. 2019;53(1):505–530.
52. Madhu K, Madhu R, Rethesh T. Broodstock development, breeding, embryonic development and larviculture of spine-cheek anemonefish, *Premnas biaculeatus* (bloch, 1790). *Indian J Fish*. 2012;59(1):65–75.
53. Salis P, Roux N, Lecchini D, Laudet V. The post-embryonic development of *Amphiprion perideraion* reveals a decoupling between morphological and pigmentation changes. *Cybium*. 2018;42(4):309–312.
54. Kelsh RN, Brand M, Jiang YJ, et al. Zebrafish pigmentation mutations and the processes of neural crest development. *Development*. 1996;123:369–389.
55. Barth P, Berenshtein I, Besson M, et al. From the ocean to a reef habitat: how do the larvae of coral reef fishes find their way home? A state of art on the latest advances. *Vie Milieu*. 2015;65(2):91–100.
56. Roux N, Logeux V, Trouillard N, et al. A star is born again: methods for larval rearing of an emerging model organism, the false clownfish *Amphiprion ocellaris*. *J Exp Zool Part B Mol Dev Evol*. 2021;jez.b.23028. <https://doi.org/10.1002/jez.b.23028>.

## ORCID

Pauline Salis  <https://orcid.org/0000-0002-5690-3714>

Natacha Roux  <https://orcid.org/0000-0002-1883-7728>

Vincent Laudet  <https://orcid.org/0000-0003-4022-4175>

## SUPPORTING INFORMATION

Additional supporting information may be found online in the Supporting Information section at the end of this article.

**How to cite this article:** Salis P, Lee S, Roux N, Lecchini D, Laudet V. The real Nemo movie: Description of embryonic development in *Amphiprion ocellaris* from first division to hatching. *Developmental Dynamics*. 2021;250(11): 1651–1667. <https://doi.org/10.1002/dvdy.354>